2014 SNMMI Highlights Lecture: Neuroscience

From the Newsline Editor: The Highlights Lecture, presented at the closing session of each SNMMI Annual Meeting, was originated and presented for more than 33 years by Henry N. Wagner, Jr., MD. Beginning in 2010, the duties of summarizing selected significant presentations at the meeting were divided annually among 4 distinguished nuclear and molecular medicine subject matter experts. The 2014 Highlights Lectures were delivered on June 11 at the SNMMI Annual Meeting in St. Louis, MO. The first presentation is included here; others will appear later this year. Nicolaas I. Bohnen, MD, PhD, spoke on neuroscience highlights. Note that in the following presentation summary, numerals in brackets represent abstract numbers as published in The Journal of Nuclear Medicine *(2014;55[suppl 1]).*

It is my distinct privilege to summarize the highlights of the neuroscience presentations from the SNMMI Annual Meeting, covering the areas of basic neuroscience, clinical neurology, and psychiatry. At this meeting, the Kuhl–Lassen Award, the major award given by the Brain Imaging Council, went to Osama Sabri, MD, PhD, from Leipzig University (Germany). The Kuhl–Lassen Award is given annually to recognize a scientist who has made outstanding contributions and whose research in and service to the discipline of functional brain imaging is of the highest caliber. Dr. Sabri has been a key researcher in European studies of ^{18}F-florbetaben, the amyloid-β (Aβ) ligand that received recent approval from the U.S. Food and Drug Administration (FDA). He is also in the forefront of research in PET/MR imaging of the brain and in the development of a new ligand, ^{18}F-flubatine, to study α4β2-nicotinic acetylcholine receptors (α4β2-nAChRs) in Alzheimer disease (AD).

It is also my privilege to recognize the young and very talented scientists honored at the Brain Imaging Young Investigators Awards session at this meeting. The winner was Dustin Wooten, PhD, who, with colleagues at Harvard Medical School and Massachusetts General Hospital (Boston) and the Massachusetts Institute of Technology (Cambridge), reported on "Occupancy and functional response to D_1 receptor ligands assessed by concurrent PET/fMRI" [30]. The second place award went to Matthias Brendel, PhD, who, with colleagues at the University of Munich (Germany), Tohoku University (Sendai, Japan), and the German Center for Neurodegenerative Diseases (Munich), reported on "PET imaging of tau pathology in a transgenic mouse model using [^{18}F]THK-5117" [28]. The third-place award went to Phillip Hsu, who, with colleagues from Washington University (St. Louis, MO), reported that "Longitudinal amyloid deposition is associated with changes in cortical thickness and white matter integrity in cognitively normal adults" [33].

Dementia and Neurodegenerative Disease

A major focus for neuroscience for the last several years has been on dementia and neurodegenerative conditions, and this continues to be true. We now have 3 Aβ PET ligands approved by the FDA: ^{18}F-florbetapir, ^{18}F-flutemetamol, and ^{18}F-florbetaben. One of the largest studies correlating PET findings with postmortem analyses (a correlation required by the FDA for approval) was presented at this meeting by Seibyl et al. on behalf of the Florbetaben Study Group, including authors from the United States, Germany, Japan, and Australia. In "A negative florbetaben PET scan reliably excludes amyloid pathology as confirmed by histopathology" [243], these authors reported on 74 patients imaged with ^{18}F-florbetaben PET shortly before the end of life (Fig. 1), followed by postmortem examination. Scans from 46 of the 47 patients determined at postmortem to be Aβ-positive were also correctly read on PET as positive; scans from 24 of the 27 subjects without Aβ were correctly read as negative; 24 of 25 scans read as negative were correctly assessed. Sensitivity, specificity, and negative predictive values were 98%, 89%, and 96%, respectively, making it a very useful ligand for clinical practice. The presence of other neuropathologies did not influence the assessment of scans in this study.

Nicolaas I. Bohnen, MD, PhD

As we know, Aβ deposition in AD does not happen overnight. It is a slowly evolving process that we now believe extends 15 or more years before conventional symptomatic presentation. This has led to the development of new clinical diagnostic criteria for AD, in which Alzheimer dementia is only the end-stage of a slowly evolving disease. The challenge is to focus on the clinically silent and prodromal stages of AD, when patients are developing Aβ plaques in the brain but remain cognitively normal. The National Institute on Aging and the Alzheimer's Association have proposed new presymptomatic diagnostic criteria as a first step in this focus, with stage 1 labeled "asymptomatic amyloidosis," stage 2 as "amyloidosis plus neurodegeneration," and stage 3 as "amyloidosis plus neurodegeneration plus subtle cognitive decline," fol-

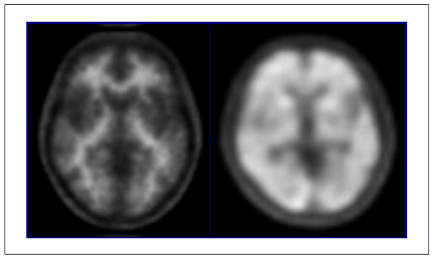

FIGURE 1. ^{18}F-florbetaben PET images negative (left) and positive (right) for Aβ correlated closely with postmortem pathology findings.

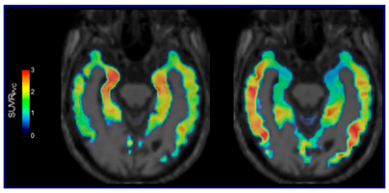

FIGURE 2. Tau and Aβ pathologies in AD visualized by, respectively, ^{18}F-THK5117 (left) and ^{11}C-PiB PET (right). ^{18}F-THK5117 retention was correlated with severity of dementia and brain atrophy in AD patients.

lowed by mild cognitive impairment (MCI) and then Alzheimer dementia. PET is an essential element in providing evidence to differentiate among these presymptomatic stages. Vlassenko et al. from Washington University (St. Louis, MO) reported on "Relationship between brain Aβ deposition and cerebrospinal fluid (CSF) Aβ42 several years prior to amyloid positivity" [188]. They studied patients between the ages of 50 and 70 years who had initially negative ^{11}C-Pittsburgh compound B (^{11}C-PiB) Aβ scans and followed these patients closely for several years. When looking at those who converted from a negative to positive Aβ scan during the follow-up period, the researchers found intriguing results. CSF changes for Aβ42 were already evident at the time of the original negative scan in individuals who would convert 2 or 3 years later to a positive Aβ scan. They concluded that reductions in CSF Aβ42 are coupled with Aβ deposition throughout the process of Aβ accumulation and that this process appears to begin years before reaching the global brain threshold for Aβ positivity. This highlights the fact that in this clinically silent phase of the disease, much is happening in the brain—and we now have tools to more fully investigate this activity.

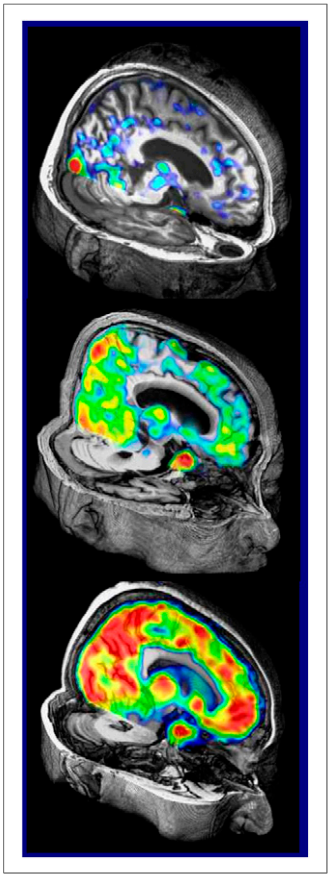

FIGURE 3. ^{11}C-PBB3 binding in AD and non-AD tauopathies. Uptake in: (top) healthy elderly individual; (middle) individual with AD-related MCI; (bottom) individual with AD. The spectrum of ^{11}C-PBB3 binding correlates with severity of clinical symptoms in individuals with AD and AD-related MCI.

Aβ accumulation is, of course, only half of the pathology needed to make a postmortem diagnosis of AD. The other pathology is tau neurofibrillary tangle deposition. At this meeting we heard reports on promising new tracers with which to study these tangles in the living brain. Okamura et al. from Tohoku University Hospital and School of Medicine (Sendai, Japan) reported on "In vivo selective imaging of tau pathology in AD with ^{18}F-THK5117" [136]. This novel PET tracer selectively labels neurofibrillary tangles in the AD brain. AD patients showed retention of the tracer more in the medial than lateral temporal cortices (Fig. 2), areas known to contain high concentrations of tau deposits. ^{18}F-THK5117 retention was correlated with the severity of dementia and brain atrophy in these patients. These findings suggest that ^{18}F-THK5117 PET would be useful for noninvasive evaluation of tau pathology in AD patients and could perhaps lead to a better understanding of the pathophysiology of AD.

Suhara et al. from the National Institute of Radiological Sciences (Chiba-shi, Japan) reported on "In vivo tau PET imaging using [^{11}C]PBB3 in AD and non-AD tauopathies" [1824]. These authors very nicely showed that we can use this ligand to track patients from MCI through severe dementia. Figure 3 shows that the intensity of tracer uptake correlated well with disease progression in terms of cognitive impairment. The authors also noted that ^{11}C-PBB3 binding has the potential to increase our understanding of tau protein–related neurologic manifestations in corticobasal syndrome, progressive supranuclear palsy, and frontotemporal dementia.

New Technologies and Ligands

Another major new field highlighted in many sessions at this meeting was that of PET/MR imaging in brain studies. Bohn et al. from the Technische Universität München (Germany) reported on "Simultaneous ^{18}F-FDG PET, pulsed arterial spin labeling (PASL) MRI and structural MRI in neurodegenerative dementia: a PET/MR study" [411]. They showed converging and overlapping patterns affecting both glucose metabolism and changes in blood flow (Fig. 4). They also showed that PASL MR imaging delivers results comparable to those with ^{18}F-FDG PET in patients with neurodegenerative AD. This highlights a proof of concept that with PET/MR imaging we may develop "one-stop shopping" for dementia diagnosis, with the ability to simultaneously assess function and anatomy.

We are always hoping for a cure for neurodegenerative diseases such as Parkinson disease and amyotrophic lateral sclerosis (ALS). To better study promising stem cell applications in these diseases we need markers that can monitor the fate of these cells once grafted in the brain. Lewis et al. from the University of Wisconsin (Madison) reported on "DMT1, a novel PET/MR reporter protein for neural stem cell tracking" [60]. These authors showed transfection of human stem cells with a divalent metal transporter that has both a manganese MR agent as well as ^{52}Mn, a PET ligand. The animal images in Figure 5 show the results of simultaneous in vivo imaging with the PET marker and the MR agent. This technique holds promise for dual-modality cell tracking in the central nervous system (CNS).

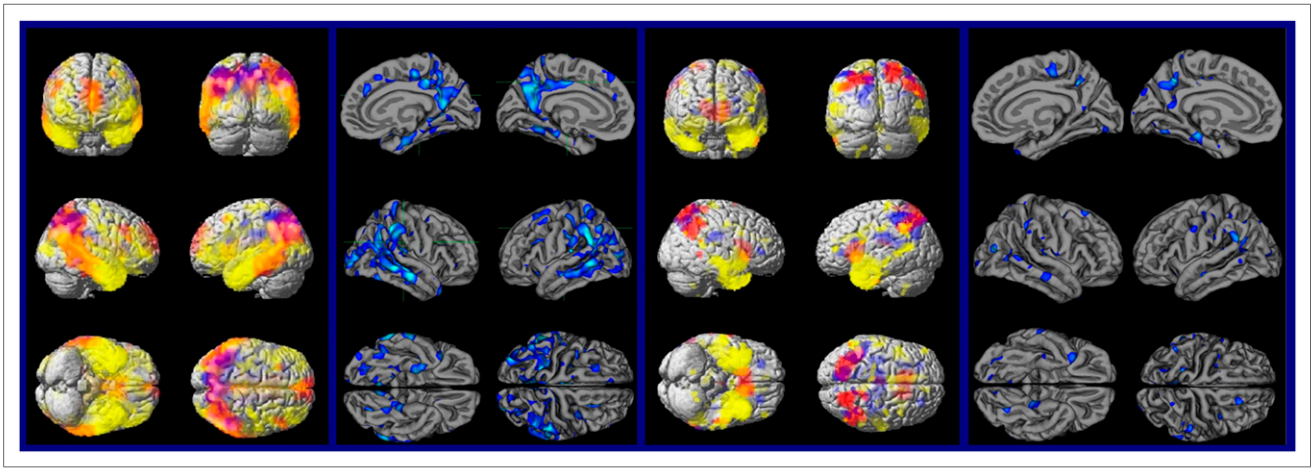

FIGURE 4. Coregistered color-coded statistical parametric mapping images (multicolored images) and pulsed arterial spin–labeled (PASL) MR images (blue and gray images) acquired in patients with (left 2 image blocks) AD and (right 2 image blocks) MCI. T1-weighted magnetization–prepared rapid acquisition gradient echo MR (yellow); PASL MR (blue); ^{18}F-FDG PET (red).

Nabulsi et al. from Yale University (New Haven, CT) and UCB Pharma SA (Brussels, Belgium) reported on "^{11}C-UCB-J: a novel PET tracer for imaging synaptic vesicle glycoprotein 2A (SV2A)" [355]. This is a much-needed tracer in the field of epilepsy for imaging and quantifying synaptic vesicle glycoprotein 2A activity. These researchers reported on initial analyses and dosimetry. Figure 6 shows excellent uptake in studies in rhesus monkeys, as well as very specific blocking of the ligand by the anti-epileptic agent levetiracetam. The authors concluded that ^{11}C-UCB-J is suitable for PET imaging of SV2A in nonhuman primate brains and reported that human studies are underway.

For many years in neuroscience we have focused on what is called the "first messenger" system: the binding of a neurotransmitter to a receptor. Much more is happening *within* the cell, and these processes are referred to as the "second messenger" system. It is quite intriguing to see that we now have ligands that bind intracellularly to the elements and enzymes of the second messenger system. For example, Niccolini et al. from the Imperial College London, King's College London, the UCL Institute for Neurology, and Imanova (all in London, UK) reported on "Brain phosphodiesterase 10A (PDE-10A) density in early premanifest Huntington's disease (HD) gene carriers" [32]. The authors used ^{11}C-IMA-107 PET imaging to study a unique cohort of early premanifest HD gene carriers to investigate the expression of PDE-10A (one of the enzymes needed in the conversion of cyclic adenosine monophosphate [cAMP] to AMP). They quantified the availability of PDE-10A in the brains of 12 early premanifest HD gene carriers with a mean of 25 years (range, 17–43 years) before the pre-

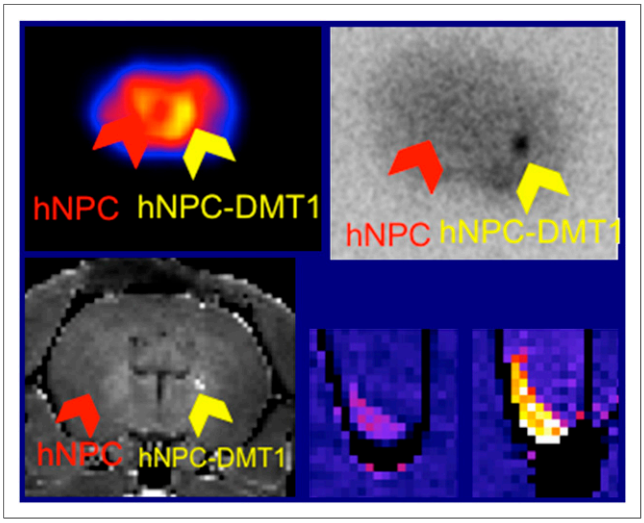

FIGURE 5. Studies with ^{52}Mn-DMT1, a novel PET/MR agent, tracking transfected human stem cells in mice. Top: Ex vivo PET (left) showed tracer uptake in transfected cells, confirmed by autoradiography (right). Bottom: In vivo (left) and in vitro (right) MR imaging showed increased T1 relaxation rate in areas of uptake of a manganese MR agent.

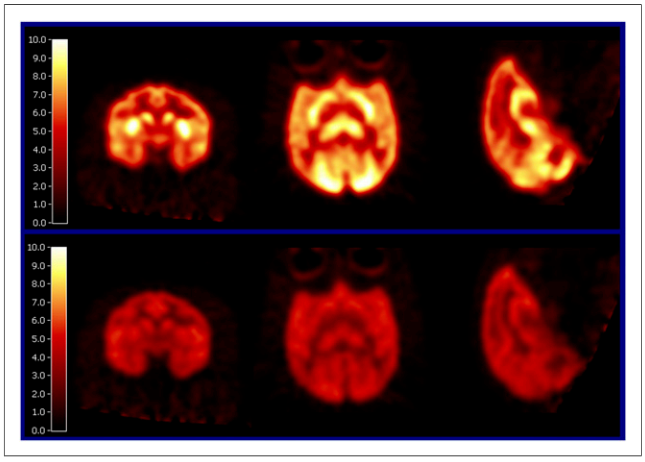

FIGURE 6. ^{11}C-UCB-J PET imaging of synaptic vesicle glycoprotein 2A (upper row). Blocking with 10 mg/kg levetiracetam yielded ~65% receptor occupancy in nonhuman primate brain (bottom row).

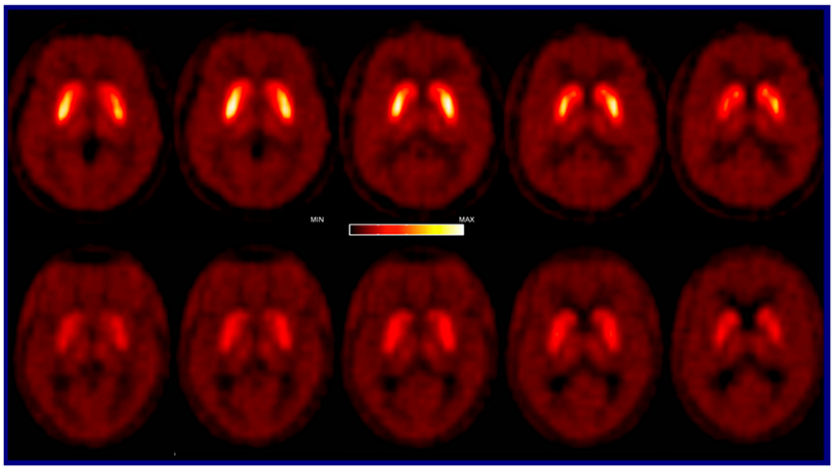

FIGURE 7. ^{11}C-IMA-107 binding in the striatum in healthy controls (top row) was greatly decreased in early premanifest Huntington disease gene carriers (bottom row).

dicted onset of clinical symptoms and in 12 matched healthy controls. They found that although early premanifest HD gene carriers were clinically normal, ^{11}C-IMA-107 PET revealed bidirectional changes in PDE-10A expression, with 17%–33% decreases in striatum, 26% decreases in globus pallidus, and 35% increases in motor thalamic nuclei compared to the healthy controls (Fig. 7). This opens up a new area of promise for treatment in the prodromal phase in this disorder.

We also have new ligands with which to study oxidative stress based on mitochondrial dysfunction. ALS, for example, is a debilitating motor neuron disease with poor clinical outlook and for which novel radioligands are needed for insight into disease pathogenesis and progression. Okazawa et al. from the University of Fukui and Fukui Prefectural University (both in Eiheiji-cho, Japan) reported on "Evaluation of cerebral oxidative stress in ALS using ^{62}Cu-ATSM PET" [1831]. Analyses showed significantly greater accumulation of this tracer in bilateral motor cortices and in the right parietal cortices of ALS patients than in healthy controls (Fig. 8). Standardized uptake values in bilateral motor cortices of ALS patients were also significantly higher. The results were inversely correlated with clinical ratings of severity of disease in ALS patients.

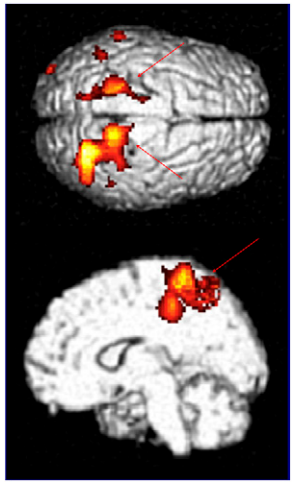

FIGURE 8. ^{62}Cu-ATSM PET and cerebral oxidative stress in ALS. Statistical parametric mapping image analysis, with medial motor cortices showing significantly higher accumulation of tracer in patients with ALS.

Barret et al. from Molecular NeuroImaging LLC (New Haven, CT) and UCB Pharma SA (Brussels, Belgium) reported on "In vivo assessment of [^{18}F]MNI-444 in human brain: a novel adenosine 2A (A_{2A}) receptor PET tracer" [356]. The A_{2A} receptor, as a binding substrate for caffeine, also has significant clinical implications for disorders such as Parkinson disease. These researchers provided the first full validation in humans of this ^{18}F-labeled PET tracer for A_{2A}, allowing noninvasive analysis over 90 minutes using the cerebellum as a reference region" (Fig. 9).

Brain Tumors

Participants in the SNMMI Annual Meeting presented a number of interesting ligands with which to target the pathology of tumors, as well as new information on the many radioisotopes that can be used to label these agents. For example, Wehrenberg-Klee et al. from Massachusetts General Hospital (Boston) reported on "A F(ab)'2-based epidermal growth factor receptor (EGFR)–targeted PET probe for glioma imaging" [1793]. ^{64}Cu-DOTA-cetuximab-F(ab')2 binds to EGFR, which is expressed on the surface of 40%–60% of glioblastoma multiforme cells. The animal model images in Figure 10 show a very high initial tumor-to-background tissue ratio, with significant reduction after cetuximab administration. Images after partial and complete resection show the specificity of the probe for tumor persistence after surgery.

A ligand for angiogenesis studies was presented by Iagaru et al. from Stanford Hospital and Clinics (CA), who reported on "^{18}F-FPPRGD2 PET/CT evaluation of patients

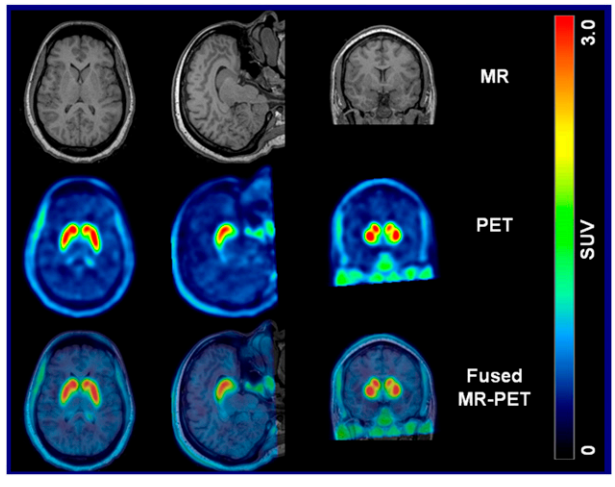

FIGURE 9. ^{18}F-MNI-444 PET as an adenosine 2A receptor tracer: MR (top row), PET, (middle row), fused MR/PET (bottom row).

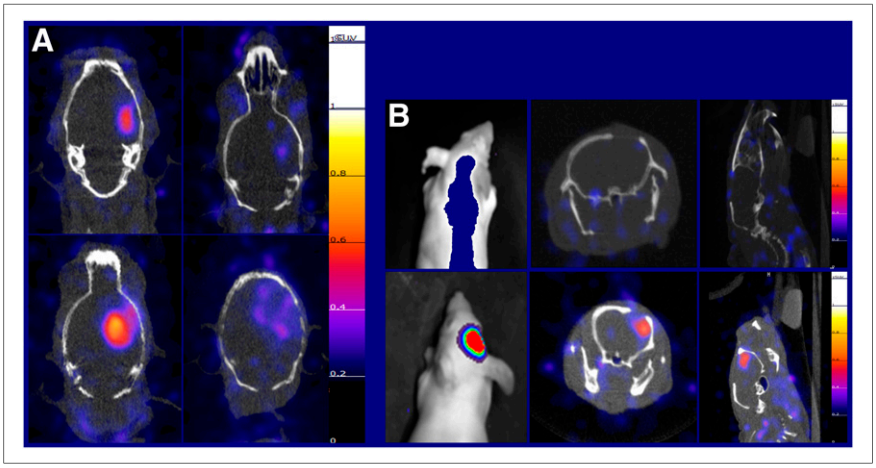

FIGURE 10. ^{64}Cu-DOTA-cetuximab-F(ab')2 PET glioma imaging in a mouse model. (A) Very high tumor-to-background ratio (left column) and significant reduction in uptake after cetuximab administration (right column). (B) Bioluminescence imaging, PET/CT, and sagittal PET/CT (left to right) at complete (top row) and partial (bottom row) resection showed the specificity of the probe.

with suspected recurrence of glioblastoma multiforme" [31] after treatment with bevacizumab. These authors showed that response could be predicted in as little as 1 week after treatment. On the left in Figure 11 are images from a participant who showed only a 4.8% reduction in uptake at 1 week; on the right is a patient who showed a 59.8% reduction at 1 week. The first patient died 4 months after treatment; the second was stable at 27 months.

Hall et al. from the University of Wisconsin and Novelos Therapeutics (both in Madison, WI) reported on "Comparison of MRI and ^{124}I-CLR1404 PET/CT in primary and metastatic brain tumors" [525]. This radiolabeled phospholipid ether analog enters malignant cells via membrane lipid rafts and is overexpressed in malignant cells. In more than 50 preclinical models, including gliomas, the researchers found tumor-specific uptake and prolonged retention of this tracer. The tracer is also suitable for isoteric iodine substitution, with ^{124}I for molecular/PET imaging and ^{131}I for therapy. Related optical imaging agents are also being developed. Figure 12 shows that the tracer not only picks up the primary CNS gliomas but also CNS metastases from non–small cell lung cancer.

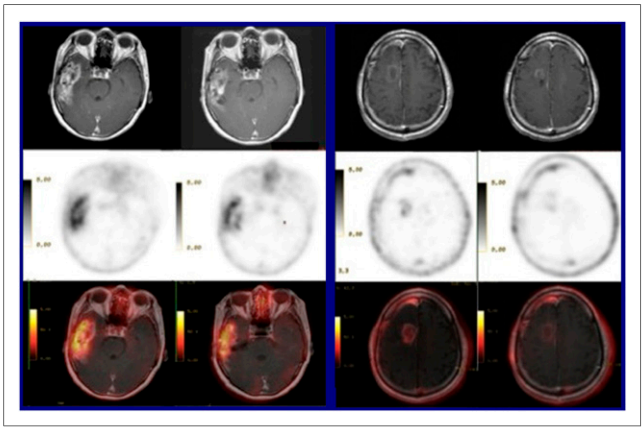

FIGURE 11. ^{18}F-FPPRGD2 PET/CT in 2 patients with suspected recurrence of glioblastoma multiforme after treatment with bevacizumab. Images show (top to bottom) MR, ^{18}F-FPPRGD2 PET, and fused PET/MR images before (left) and after (right) initiation of treatment. The patient in the left block of images showed only a 4.8% reduction in uptake at 1 week and died 4 months later. The patient in the right block of images showed a 59.8% reduction at 1 week and was stable at 27 months.

Psychiatry

Although the number of submissions in this category was relatively low at this meeting, their high quality was impressive. Meyer et al. from the University of Leipzig (Germany) reported on "α4β2-nAChR binding in acute unmedicated major depressive disorder (MDD): a 2-[^{18}F]F-A-85380 PET study" [83]. These researchers found significantly lower corticolimbic and paralimbic α4β2-nAChR availability in acute unmedicated MDD patients than in healthy controls, and these decreases were directly correlated with severity of disease (Fig. 13). Such results provide new windows on potential treatments for depression.

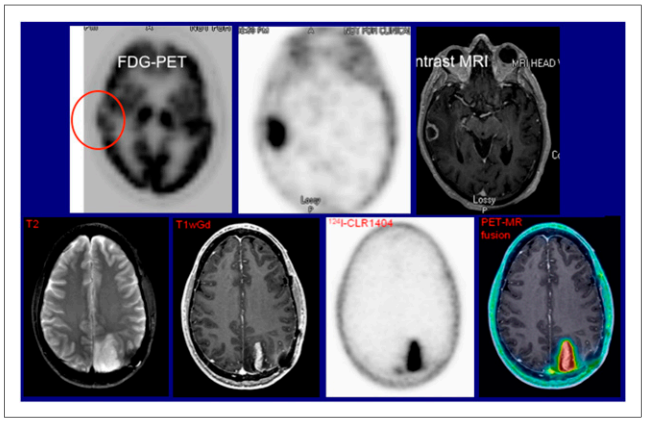

FIGURE 12. ^{124}I-CLR1404 (also called NM404) PET studies. Top row: patient with non–small cell lung cancer. Left to right: ^{18}F-FDG PET, ^{124}I-CLR1404 PET, and contrast MR imaging showing striking image contrast differences between low ^{18}F-FDG and very intense phospholipid ether analogue uptake in right temporal metastasis. Bottom row: patient with World Health Organization stage III glioma. Left 2 images: T2-weighted and contrast-enhanced MR images show wide area of edema but more limited area of abnormal MR contrast enhancement in left parieto-occipital glioma. Right 2 images: phospholipid ether analogue PET shows intense tracer uptake, and fused PET–contrast MR image shows larger area of abnormal PET tracer uptake than MR contrast enhancement in the tumor.

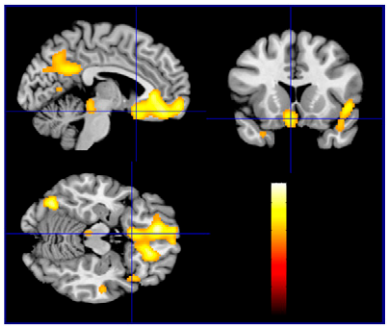

FIGURE 13. 2-[^{18}F]F-A-85380 PET in patients with acute unmedicated major depressive disorder (MDD). Statistical parametric images show areas of decreased α4β2 nicotinic receptor binding (depicted in yellow) in corticolimbic (orbitofrontal), limbic regions, and the posterior cingulum in patients with MDD compared to control subjects.

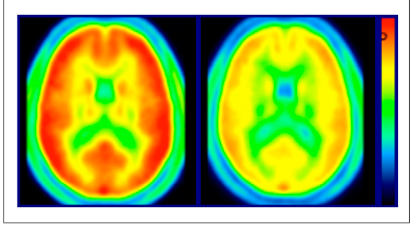

FIGURE 14. ^{11}C-(*R*)-rolipram PET images in healthy controls (left) and unmedicated patients with major depressive disorder (MDD, right). Severe decreases in binding were seen in MDD patients, but these decreases normalized after ~8 weeks of selective serotonin reuptake inhibitor therapy.

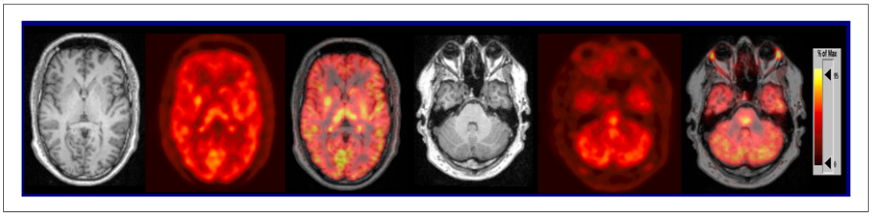

FIGURE 15. ^{11}C-MRB PET and stress response in obesity. Selected MR, ^{11}C-MRB PET, and fused PET-MR transaxial image slices centered at subcortical gray structures (basal ganglia, thalami; first 3 images from left) and brainstem at the level of the locus ceruleus (3 images from right), showing regional cerebral noradrenaline transporter availability. Correlational analysis between regional cerebral PET noradrenaline transporter availability, stress hormone responsiveness, and behavioral ratings of impulsiveness showed evidence of higher noradrenergic tone (higher arousal) in obese individuals, factors related to an altered stress response and impulsive behavior.

The imaging of the second messenger system as a novel way to understand brain disease was mentioned earlier in the context of HD. Another example was presented by Fujita et al. from the National Institute of Mental Health (Bethesda, MD) and Johnson & Johnson (New Brunswick, NJ), who reported on "Cyclic AMP cascade in MDD imaged with ^{11}C-(*R*)-rolipram: downregulation in unmedicated patients and normalization by antidepressant treatment" [81]. In unmedicated MDD patients, tracer uptake was severely reduced in comparison with uptake in healthy controls (Fig. 14). However, the use of antidepressants normalized uptake in MDD patients, with increases in ^{11}C-(*R*)-rolipram binding correlating with symptom improvement. This PET study of a second messenger system in MDD confirms the cAMP theory of depression and of antidepressant action and suggests that MDD can be treated with PDE-4 inhibitors.

Hesse et al. from the University of Leipzig (Germany) in collaboration with the New York University School of Medicine (NY) reported that "Stress response and impulsivity are related to noradrenaline transporter availability in obesity" [86]. The researchers used ^{11}C-MRB, a norepinephrine transporter ligand, to investigate whether central noradrenaline transporter availability is altered in relation to stress response in extremely obese individuals as a pathomechanism in obesity (Fig. 15). They used the dexamethasone suppression test to determine stress hormone responsiveness in obese individuals. Their data suggest a pathomechanism of a higher noradrenergic tone (higher arousal) in obesity, which is related to an altered stress response and impulsive behavior. This provides new insights on why obese individuals may maintain obesity despite interventions.

Conclusion

The neuroscience presentations at this meeting were quite intriguing and introduced many new leads for diagnosis and monitoring of treatments, as well as leads for development of new treatments for patients with CNS disorders.

Nicolaas I. Bohnen, MD, PhD
University of Michigan Medical School and
Veterans Affairs Medical Center
Ann Arbor, MI